Damage Analysis of Hybrid Composites Under Multi-Impact Loads: an Experimental and Numerical Study

Bruno Matteo[1,a*], Carrino Luigi[1,b], Donadio Federica[1,c], Esposito Luca[1,d],
Lopresto Valentina[1,e], Ilaria Papa[1,f], and Antonio Viscusi[1,g]

[1]Department of Chemical, Materials and Production Engineering,
University of Naples Federico II, Piazzale V. Tecchio 80, 80125 Napoli, Italy

[a]matteo.bruno@unina.it, [b]luigi.carrino@unina.it, [c]federica.donadio@unina.it,
[d]luca.esposito2@unina.it, [e] valentina.lopresto@unina.it, [f]ilaria.papa@unina.it,
[g]antonio.viscusi@unina.it

Abstract. Laminated composite structures are subjected to impact damage during maintenance, manufacturing operations and their life service. Driven by the necessity to value damage tolerance and durability of composite materials, an analysis of multi-hit impact is conducted to reproduce the real service conditions. Despite many studies in the literature investigated the properties of composites at low impact velocity, in contrast the behavior of the hybrid configuration, especially at repeated impacts, result still little known. This work presents an experimental and numerical study of the dynamic behavior at the repeated low-velocity impact of a carbon and glass fibers hybrid composite laminate.

Introduction

The anisotropic and heterogeneous character of Fiber Reinforced Polymers (FRP), together with their capability to offer high mechanical performance in terms of stiffness and strength in reduced weight, spread their application in the industrial field both for structural and non-structural purposes [1, 2, 3, 4, 5]. This drove many studies to investigate the FRP mechanical response under quasi-static and dynamic load conditions [6, 7, 8, 9].Since not easily identifiable by visual inspection, or barely visible on the component surface, the damage from foreign object impact resulted to be a critical condition for this class of materials. Even when undetectable, the damage consequent to impact loads, can significantly reduce the laminate strength by promoting material failure also under operating loads [10, 11, 12]. The FRP strength and stiffness reduction, particularly due to repeated Low-Velocity Impact (LVI), resulted to be a consequence of stacked delamination on the ply-to-ply interfaces and resin or fiber damage interesting the plies. This variety of damage typology, induced by the impact loads on composites, resulted complicated to predict due to the non-homogeneous and anisotropic nature of these materials. Due to the prominence of the issue, a variety of studies were dedicated to deepening the problem and several approaches were proposed in literature over the years to mitigate the damage resulting from LVI in FRP materials and estimate the after-impact fitness for service [13, 14].More recently, with the purpose to tailor the impact response and to maximize the energy absorption of the FRPs, several methods have been developed. A feasible solution was found in the hybridization of laminates, profiting from the distinctive properties of different fibers in the same matrix [15, 16, 17, 18, 19]. In this regard, the adoption of inexpensive glass fibers represents an appropriate option, especially if coupled with more performing and expensive carbon fibers. Many studies in literature investigated the hybrid glass/carbon composite laminates evidencing an increased damage tolerance if compared to the full carbon counterparts. Improvements in maximum bearable load and energy absorption capability were associated with the increasing of the glass fiber fraction and resulted to be a direct consequence of the stacking sequence [16, 17, 20, 21, 22]. Thus, a reduction of the LVI damage, which means increased residual strength, can be obtained through a proper design of the laminate layup.

Driven by the necessity to evaluate damage tolerance and durability of the composite under LVI depending on the stacking sequence, many experimental and numerical investigations have been con-

ducted in literature [23, 24, 25, 26, 27]. In contrast, the behavior of the hybrid configurations, especially at repeated impacts, is still little known. Therefore, in this study, the response of a glass/carbon alternated hybrid laminate was both experimentally and numerically investigated under repeated LVI with the purpose to characterize the damage typology and estimate the fitness for service capability of the impacted laminate.

Materials and Methods

In the following sections, the studied glass/carbon hybrid laminate will be described, and the manufacturing procedure deepened. Then the repeated impact tests conducted, and the experimental set-up will be presented. Subsequently, the numerical approach adopted to achieve the model will be described and the choice of the parameters motivated.

Experimental Methodology. The composite laminate considered in the present study presented a $([G_2C]_5G_2)$ stacking sequence obtained by alternating two plies of glass every ply of carbon for a total of 17 plies $[0°/90°]$ oriented. The laminate was manufactured with a vacuum infusion technique by using vinyl-ester *Crystic VE 679PA* resin and woven fabrics for the glass and carbon reinforcement with an areal weight of about $300 g/m^2$, respectively provided by *Castro Composite* and *Mike Composite*. The resulting composite laminate showed a nominal thickness of $t = 3.5 \pm 0.25 mm$ and a measured fiber volume fraction of about $V_f \simeq 58\%$. A descriptive sketch of the stacking sequence configuration is shown in Fig. 1 (a).
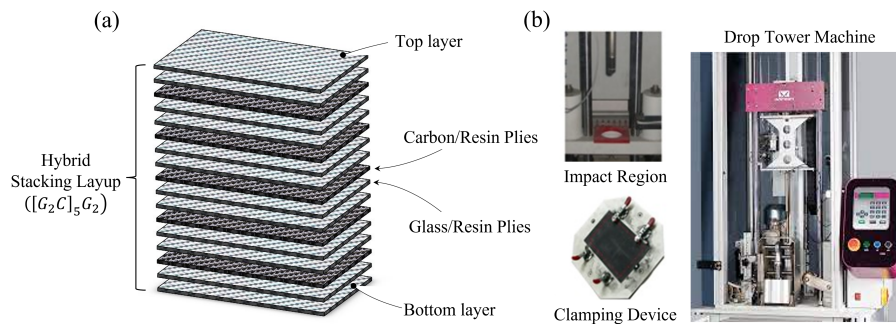

Fig. 1: A descriptive sketch of the studied hybrid stacking layup (a) and experimental equipment (b).

The experimental campaign consisted of the repetition of three impact tests at the same energy level, was conducted according to the *ASTM D7136* international standard by using a drop tower machine *Instron* equipped with an anti-rebound system reported in Fig. 1 (b). To obtain the desired impact energy, equal to 10J, a hemispheric impactor with a diameter of 19.8 mm and a total mass of 3.62 kg was dropped from a height of about 281 mm. The impacted panel consisted of a 100 x 150 mm rectangular plate cutting by the laminate and positioned on the testing area by clamping all the edges. After each impact event, the ultrasonic inspection was executed to evaluate the evolution of the damage extension within the panel. Information about impact force, panel deflection and energy absorption trend over impact time were estimated and, as a result of the ultrasonic inspection, the total damaged area was measured for each of the three-impact repetitions.

Numerical Methodology. The normal impact of the impactor on the panel sample was numerically reproduced through an explicit calculation method on the commercial Finite Element Analysis (FEA) software *ABAQUS*. The symmetry of the geometry, loads and constraints, with respect to the 1-3 and 2-3 planes, allowed to schematize the problem as a symmetric quarter model, as schematically reported in Fig. 2. The impactor was modeled as an hemispherical rigid surface, meshed with 0.5 mm quadrilateral elements, and constrained by suppressing all the degree of freedom less than the falling direction displacement. On a reference point, placed on the indenter center of gravity, the total mass and the impact velocity were applied.
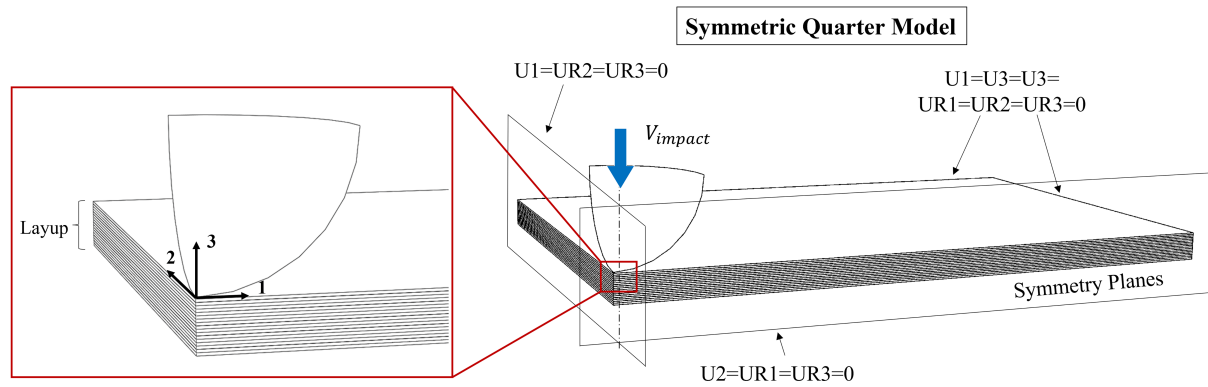
Fig. 2: Scheme of the numerical impact quarter model with highlighted the symmetry cutting planes, the laminate layup, and the applied load and constraints.

With the purpose to investigate the hybrid laminate damage evolution and the energy absorption under repeated impacts, a mesoscale approach to the panel discretization was adopted. The laminate was obtained by modeling each ply as an independent 3-dimensional geometry, adopting a continuum shell section and quadrilateral 8-nodes elements with reduced integration. To guarantee the required accuracy of the calculus, a mesh sensitivity study was conducted considering the von Mises equivalent stress and the logarithmic strain as outputs. As result, a minimum of 0.5 mm and a maximum of 2 mm element size were respectively adopted in the impact region and in the rest of the panel. The thickness of the elements was rather fixed as equals to the single ply thickness (0.234 mm). The single plies behaviour was numerically implemented adopting an orthotropic material model, whose mechanical properties were experimentally measured and here reported in Table 1, both for the glass-resin and carbon-resin plies.

Table 1: Carbon/resin and Glass/resin elastic mechanical properties.

	$E_{11}[GPa]$	$E_{22}[GPa]$	ν_{11}	$G_{12}[GPa]$	$G_{23}[GPa]$	$G_{13}[GPa]$	$\rho[kg/m^3]$
Carbon/resin	95	95	0.15	5	3	3	2000
Glass/resin	52	52	0.15	4	2.7	2.7	1800

The plies intralaminar damage was modeled through a linear stress-dependent hashin damage initiation and an energy governed damage evolution [28]. Both for glass-resin and carbon-resin plies the fracture toughness as well as the strength, as following reported in Table 2, were considered comparable in the two in-plane principal directions.

Table 2: Carbon/resin and Glass/resin in-plane Hashin damage properties.

	Tensile strength [MPa]	Compressive strength [MPa]	Shear strength [MPa]	Fracture Energy [mJ/mm^2]
Carbon/resin	950	700	80	35
Glass/resin	600	400	80	14

The laminate was obtained by stacking the plies according to the hybridization sequence of the considered composite. The resulting panel was constrained by suppressing all the degrees of freedom on the free side edges and imposing symmetry constraints, as reported in Fig. 2, to the symmetry plane edges. The interlaminar connection between the adjoining plies was modeled by adopting a surface-to-surface Cohesive Zone Model (CZM) [29, 30]. Due to the dependency of delamination just to the

matrix mechanical properties, the bilinear traction-separation law imposed to the CZM was tuned on the vinylester resin properties, as known in literature [31, 32] and here reported in Table 3.

To take into account the mutual interaction of the different modes (normal mode ad shear modes), the mixing mode delamination was implemented according to the Benzeggagh and Kenane (B-K) energy criterion, which was demonstrated to be useful when the fracture toughness of the shear directions are equals [33], as in the present case.

Table 3: CZM penalty stiffness, initiation stresses and fracture toughness properties.

Penalty stiffness	k_s	k_s	k_t
$[GPa/mm]$	100	60	60
Maximum nominal stresses	σ_n^*	σ_s^*	σ_t^*
$[MPa]$	45	60	60
Interlaminar fracture toughness	G_n	G_s	G_t
$[mJ/mm^2]$	0.54	1.2	1.2

The three 10J repeated impacts were numerically reproduced with the proposed model. The experimental contact force, panel deflection and energy absorption trends over impact time were compared to those numerically computed at the impactor center of gravity, to validate the model. The validated model was then adopted to estimate the evolution of the intralaminar and interlaminar damage as well as of the post-impact laminate residual strength as a result of each impact in relation to the hybridization sequence.

Results and Discussion

In Fig. 3, a comparison between the experimentally measured and the numerically computed, impact force to panel deflection curve, is reported for each repeated impact. A high degree of faithfulness in the numerical model results predictiveness can be observed for all the subsequent impacts, with numerical results deviation always below the 2.5% both with respect to the maximum force and maximum deflection. Also the trend of the considered parameters throughout the simulation resulted in a good correlation with the experiments, with the R-squared value between 0.85 and 0.97.
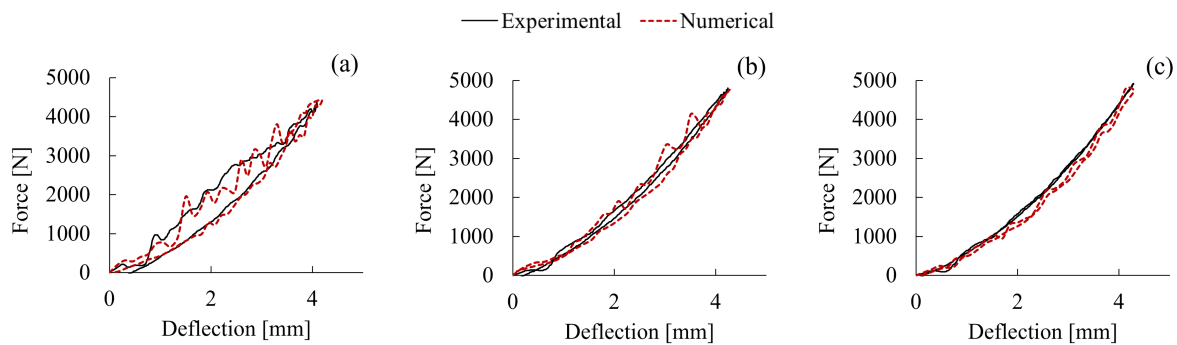

Fig. 3: Experimental and numerical comparison of impact force to panel deflection curves, for the first (a), the second (b) and the third (c) repeated 10J impact.

The presented results show an increase in both maximum impact force and panel deflection with the impact repetition. Also the panel rigidity was affected by the impact repetition, resulting in a progressive stiffness reduction. To deepen the panel absorption behavior, the experimental panel internal energy curves were reported in Fig. 4 with the numerical corresponding; once again, a good prediction of the laminate behavior can be seen for all the subsequent impact tests.
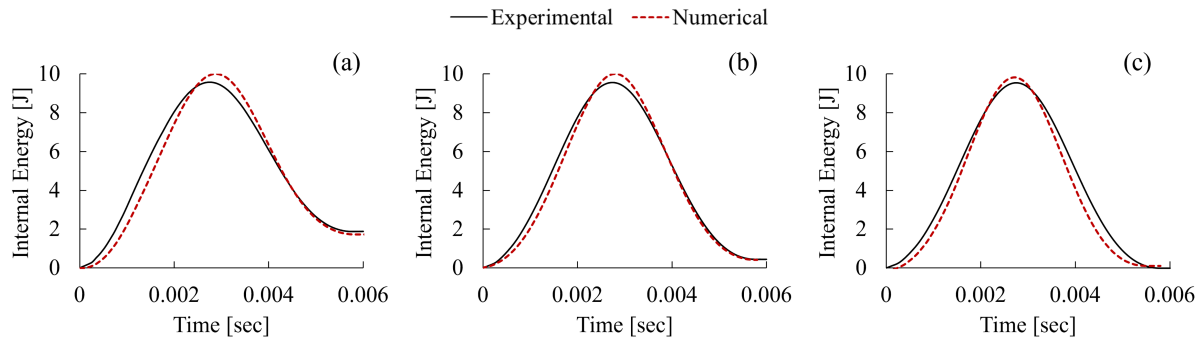
Fig. 4: Numerically computed and experimentally measured panel internal energy to impact time, for the first (a), the second (b) and the third (c) repeated 10J impact.

Values of absorbed energy, resulting from each impact, were shown in Fig. 5, together with the maximum impact force and panel deflection. The comparison between the first and the second impact showed a 10% increase in force and a 3.5% in deflection, respect to that resulted between the second and the third impact with a 2.5% increase in force and a 1% in deflection, which can be considered as a negligible difference. The lowest contact force, associated with the highest energy absorption, characterizing the first impact, suggested greater damage occurred with respect to the remaining two impacts, where the damaged panel produced higher forces, lower energy absorptions and nonsignificant variation in deflection.
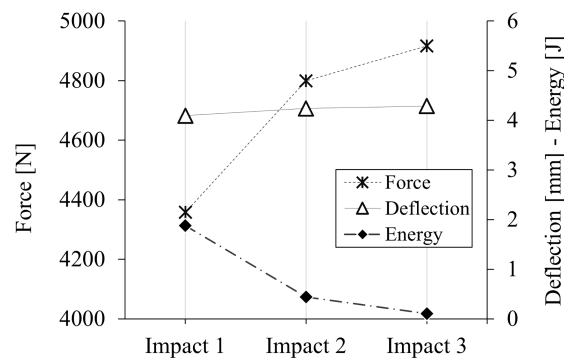

Fig. 5: Maximum contact force, maximum panel deflection and absorbed energy for each of the three repeated impact tests.

To corroborate these conclusions, after each impact event, a nondestructive ultrasonic inspection was performed on the panel to detect the damage evolution and estimate the damaged area extension. The detected damaged area, reported in Table 4, confirming the hypothesized behavior, shows the first impact produced the most extended damage with respect to the following two impacts which presented an increase in the damaged area respectively equals to 6% and 15% of the previous damage amount.

Table 4: Damaged area after each repeated impact, by ultrasonic inspection.

	Impact 1	Impact 2	Impact 3
Area $[mm^2]$	449.34	476.10	527.48

The evidenced difference, in the panel impact behavior, was thoroughly investigated thanks to the proposed numerical model, which was considered validated in the light of the high degree of experimental results predictiveness. It allowed to deepen the nature of the experimentally measured damage, as well as to characterize its evolution with the impacts repetition. In Fig. 6, the numerically
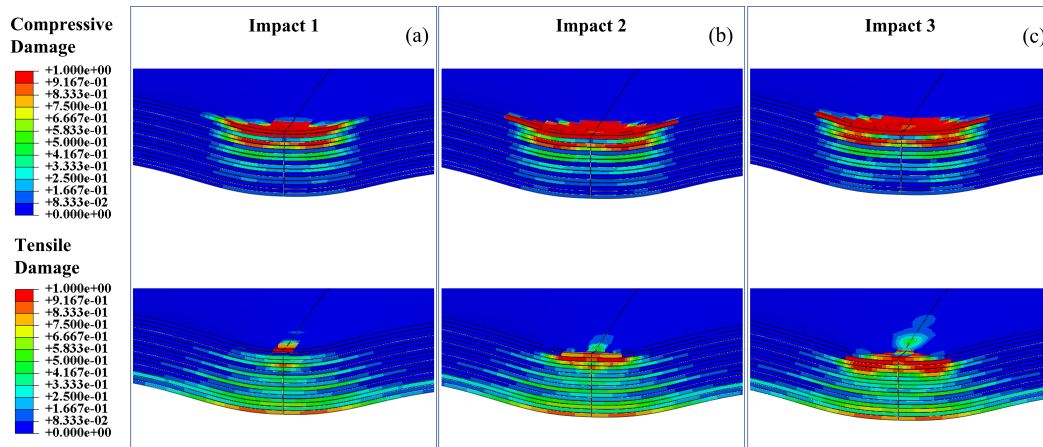
Fig. 6: Compressive and Tensile Hashin damage initiation as a consequence of the first (a), the second (b), and the third (c) repeated 10J impact.

computed tensile and compressive intralaminar damage are reported. As a result of the first impact a compressive damage initiation can be detected on the top region of the panel; mainly localized under the impactor, this damage resulted mostly as a consequence of the matrix cracking. On the contrary, the tensile damage, due to the fiber and matrix tensile failure, was localized on the bottom region of the panel. Although less extended, respect to the tensile damage, because of the greater number of completely eroded elements, the compression resulted to be the heaviest damage mechanism.

Since governed by the matrix, the distribution of the compressive damage results substantially unaffected by the hybridization sequence; while, the distribution of the fiber-governed tensile damage, has shown to more affect the glass plies with respect to the carbon plies. This behavior suggested, as already observed in literature [16], the presence of the hybrid layup reduced the damage incidence in the region that was governed by the reinforcements. By studying the evolution of both the damage type, with the impact repetition, it can be noticed the damage accumulation is always localized on the top of the panel, where an ever more extended damaged area is returned by the model. This damage, not easily detectable by visual inspection, interests the layers immediately under the impactor, by causing the complete deletion of the elements in contact with that.

To evidence this phenomenon, an experimental to numerical superficial damage comparison, after the three repeated impacts, is here reported in Fig. 7. The experimentally visible eroded region in Fig. 7(a), shows the area interested by the damage results to be smaller compared to that in greyscale numerically computed in Fig. 7(b). A damage extension wider than that observed by visual inspection also resulted from the delamination damage analysis which showed, in consequence of the first impact, a significant interlaminar damage localized on the carbon to glass plies interfaces. For the sake of brevity, only the largest delaminated interface was here reported and commented. It resulted to be the glass ply n.5 to carbon ply n.6 contact surface, showed after each impact in Fig. 8(a). This damage tends to enlarge because of the subsequent impacts as reported in Fig. 8(b) in form of delamination boundaries comparison.

This characteristic behavior did not interest all the remaining delaminated interfaces, but it was detectable only in those coupling the two different materials; precisely the glass ply n.2 to carbon ply n.3 and the carbon ply n.12 to glass ply n.13. On the contrary, all the delaminated glass to glass plies presented a reduced damage extension after the first impact and did not result affected by damage growth during the following impacts.

Conclusions

The present work aimed to investigate the dynamic behavior, at the repeated low-velocity impact, of a carbon and glass alternate hybrid laminate. For this purpose, drop impact tests were conducted at a constant impact energy level equal to 10J, and a numerical model was developed and validated on the
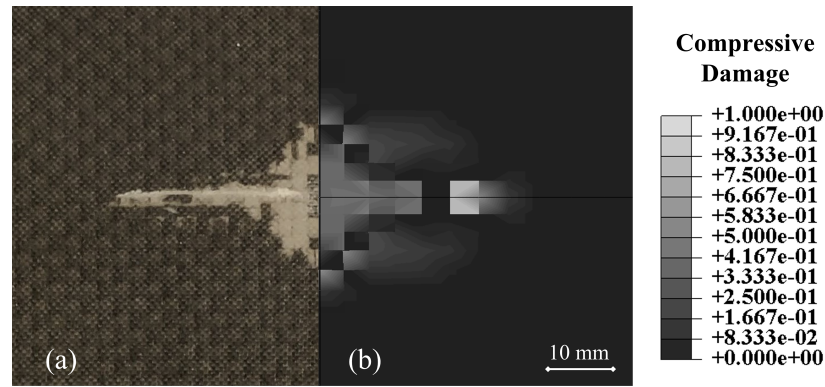
Fig. 7: Experimental (a) to numerical (b) superficial compressive damage comparison after the three repeated impacts.
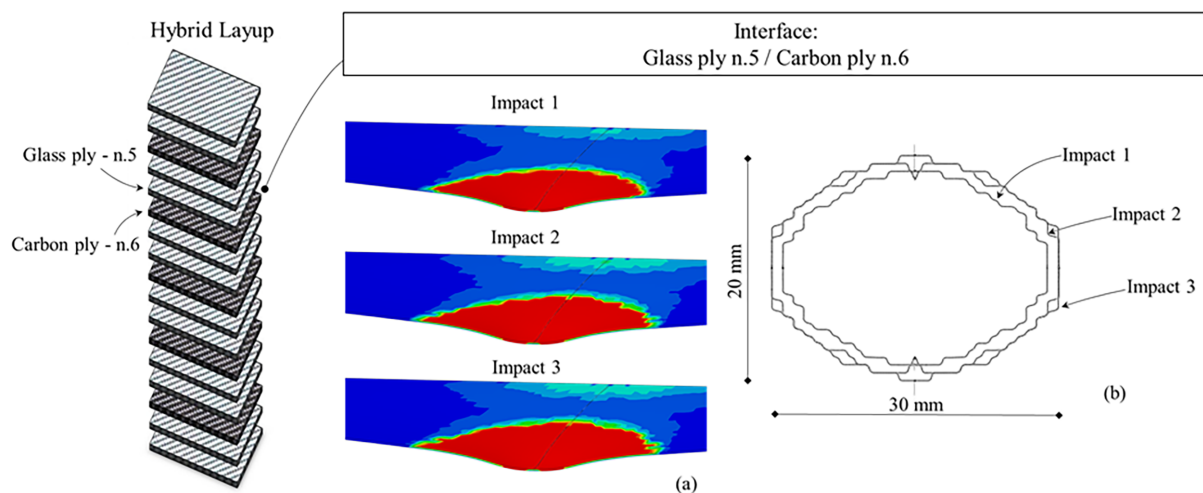

Fig. 8: Glass ply n.5 to carbon ply n.6 interface delamination (a), and delamination boundaries comparison (b) after each repeated impact.

basis of the experimental results. The discussed results allowed to deepen the nature of the damage and characterize its evolution with the impact repetition. Substantial differences were found in the panel behavior, as well as in the damage characterization, between the first and the following impacts. A 10% lower force, with respect to those measured in the last two impacts, characterize the first impact; while the deflection resulted to be not significantly influenced by the repetition. This was associated with a progressive decrease of the absorbed energy, with the first impact which resulted again in the highest absorption. As resulted from the non-destructive ultrasonic inspection that revealed the damaged area grows ever less with the repetition of the impacts. Then the numerical proposed model allowed to investigate the nature of the damage, evidencing the concomitant presence of different damage types:

- A severe intralaminar compressive damage, affecting the impact region on the top of the panel, showed a progressive growth with the impacts repetition. This damage was independent from the hybridization sequence.

- A less severe tensile intralaminar damage, localized on the bottom of the panel, showed to more affect the glass plies and resulted unaltered by the impacts followed the first one.

- The interlaminar damage, due to the first impact, mainly interested the carbon-to-glass plies interfaces, while the glass-to-glass interfaces were less affected by the delamination; evidencing an influence of the hybridization sequence into the delamination mechanisms.

- The carbon to glass plies interfaces showed a delamination enlargement due to the impact repetition; whereas the glass-to-glass interfaces were not affected by damage growth during the following impacts.

References

[1] F. Paris, K. E. Jackson, A Study of Failure Criteria of Fibrous Composite Materials, Office (March) (2001) 76.

[2] B. Soares, R. Preto, L. Sousa, L. Reis, Mechanical behavior of basalt fibers in a basalt-UP composite, Procedia Structural Integrity 1 (February) (2016) 82–89. doi:10.1016/j.prostr.2016.02.012.

[3] V. Fiore, T. Scalici, G. Di Bella, A. Valenza, A review on basalt fibre and its composites, Composites Part B: Engineering 74 (2015) 74–94. doi:10.1016/j.compositesb.2014.12.034.

[4] P. Rozylo, M. Ferdynus, H. Debski, S. Samborski, Progressive failure analysis of thin-walled composite structures verified experimentally, Materials 13 (5) (2020). doi:10.3390/ma13051138.

[5] A. Viscusi, R. D. Gatta, F. Delloro, I. Papa, A. S. Perna, A. Astarita, A novel manufacturing route for integrated 3D-printed composites and cold-sprayed metallic layer, Materials and Manufacturing Processes 0 (0) (2021) 1–14. doi:10.1080/10426914.2021.1942908.

[6] L. Esposito, G. P. Pucillo, V. Rosiello, On the geometric transferability of the delamination shear limit for CFRP laminate in bending, Theoretical and Applied Fracture Mechanics 91 (2017) 17–24. doi:10.1016/j.tafmec.2017.03.003.

[7] W. J. Cantwell, J. Morton, The impact resistance of composite materials - a review, Composites 22 (5) (1991) 347–362. doi:10.1016/0010-4361(91)90549-V.

[8] G. Lamanna, C. G. Opran, Numerical characterization of pretensioning of a hybrid joint under longitudinal load, Macromolecular Symposia 396 (1) (2021) 2100009. doi:https://doi.org/10.1002/masy.202100009.

[9] G. Lamanna, S. M. Ion, C. G. Opran, Flexural effects evaluation on hybrid joints under uniaxial tensile load, Macromolecular Symposia 396 (1) (2021) 2100007. doi:https://doi.org/10.1002/masy.202100007.

[10] M. O. Richardson, M. J. Wisheart, Review of low-velocity impact properties of composite materials, Composites Part A: Applied Science and Manufacturing 27 (12 PART A) (1996) 1123–1131. doi:10.1016/1359-835X(96)00074-7.

[11] Z. Hashin, Failure Criteria for Unidirectional Fiber Composite, Journal of Applied Mechanics 47 (June) (1980) 329–334.

[12] G. Lamanna, M. Perrella, C. G. Opran, Numerical and experimental investigation on the influence of tightening in a hybrid single lap joint, Macromolecular Symposia 396 (1) (2021) 2100010. doi:https://doi.org/10.1002/masy.202100010.

[13] A. Dogan, V. Arikan, Low-velocity impact response of E-glass reinforced thermoset and thermoplastic based sandwich composites, Composites Part B: Engineering 127 (2017) 63–69. doi:10.1016/j.compositesb.2017.06.027.

[14] R. C. Batra, G. Gopinath, J. Q. Zheng, Damage and failure in low energy impact of fiber-reinforced polymeric composite laminates, Composite Structures 94 (2) (2012) 540–547. `doi:10.1016/j.compstruct.2011.08.015`.

[15] Y. Swolfs, I. Verpoest, L. Gorbatikh, Recent advances in fibre-hybrid composites: materials selection, opportunities and applications, International Materials Reviews 64 (4) (2019) 181–215. `doi:10.1080/09506608.2018.1467365`.

[16] N. K. Naik, R. Ramasimha, H. Arya, S. V. Prabhu, N. ShamaRao, Impact response and damage tolerance characteristics of glass-carbon/epoxy hybrid composite plates, Composites Part B:Engineering 32 (7) (2001) 565–574. `doi:10.1016/S1359-8368(01)00036-1`.

[17] I. Papa, L. Boccarusso, A. Langella, V. Lopresto, Carbon/glass hybrid composite laminates in vinylester resin: Bending and low velocity impact tests, Composite Structures 232 (July 2019) (2020). `doi:10.1016/j.compstruct.2019.111571`.

[18] D. Mocerino, L. Boccarusso, D. De Fazio, M. Durante, A. Langella, M. Meo, F. Pinto, F. Rizzo, Prediction of the Impact Behavior of Bio-hybrid Composites Using Finite Element Method, ESAFORM 2021 06 (2021) 1–11. `doi:10.25518/esaform21.2651`.

[19] I. Papa, F. Donadio, V. S. Gálvez, V. Lopresto, On the low- and high-velocity impact behaviour of hybrid composite materials at room and extreme temperature, Journal of Composite Materials (2020) 00219983211047688`doi:10.1177/00219983211047688`.

[20] E. Sevkat, B. Liaw, F. Delale, B. B. Raju, Drop-weight impact of plain-woven hybrid glass-graphite/toughened epoxy composites, Composites Part A: Applied Science and Manufacturing 40 (8) (2009) 1090–1110. `doi:10.1016/j.compositesa.2009.04.028`.

[21] L. Esposito, A. Bertocco, R. Sepe, E. Armentani, 3D strip model for continuous roll-forming process simulation, Procedia Structural Integrity 12 (2018) 370–379. `doi:10.1016/j.prostr.2018.11.080`.

[22] L. Esposito, A. Bertocco, G. Cricrì, V. Rosiello, Welding-repair effect on F357-T6 aluminum castings: analysis of fatigue life, International Journal of Advanced Manufacturing Technology 102 (9-12) (2019) 3699–3706. `doi:10.1007/s00170-019-03436-4`.

[23] Y. Swolfs, Y. Geboes, L. Gorbatikh, S. T. Pinho, The importance of translaminar fracture toughness for the penetration impact behaviour of woven carbon/glass hybrid composites, Composites Part A: Applied Science and Manufacturing 103 (2017) 1–8. `doi:10.1016/j.compositesa.2017.09.009`.

[24] A. K. Bandaru, S. Patel, S. Ahmad, N. Bhatnagar, An experimental and numerical investigation on the low velocity impact response of thermoplastic hybrid composites, Journal of Composite Materials 52 (7) (2018) 877–889. `doi:10.1177/0021998317714043`.

[25] M. Sayer, N. B. Bektaş, O. Sayman, An experimental investigation on the impact behavior of hybrid composite plates, Composite Structures 92 (5) (2010) 1256–1262. `doi:10.1016/j.compstruct.2009.10.036`.

[26] F. Xu, X. Zhang, H. Zhang, A review on functionally graded structures and materials for energy absorption, Engineering Structures 171 (May) (2018) 309–325. `doi:10.1016/j.engstruct.2018.05.094`.

[27] V. Lampitella, M. Trofa, A. Astarita, G. D'Avino, Discrete Element Method Analysis of the Spreading Mechanism and Its Influence on Powder Bed Characteristics in Additive Manufacturing, Micromachines 12 (4) (2021). `doi:10.3390/mi12040392`.

[28] M. Bruno, L. Carrino, L. Esposito, V. Lopresto, I. Papa, P. Russo, A. Viscusi, A Numerical Investigation about Temperature Influence on Thermoplastic Hot-Formed Reinforced Composites Under Low-Velocity Impact 16 (2021) 1–10. `doi:10.25518/esaform21.524`.

[29] A. Turon, C. G. Dávila, P. P. Camanho, J. Costa, An engineering solution for mesh size effects in the simulation of delamination using cohesive zone models, Engineering Fracture Mechanics 74 (10) (2007) 1665–1682. `doi:10.1016/j.engfracmech.2006.08.025`.

[30] A. Turon, P. P. Camanho, J. Costa, C. G. Dávila, An Interface Damage Model for the Simulation of Delamination Under Variable-Mode Ratio in Composite Materials, Nasa/Tm-2004-213277 (NASA/TM-2004-213277) (2004).

[31] M. Soroush, K. Malekzadeh Fard, M. Shahravi, Finite element simulation of interlaminar and intralaminar damage in laminated composite plates subjected to impact, Latin American Journal of Solids and Structures 15 (6) (2018). `doi:10.1590/1679-78254609`.

[32] K. Song, C. Davila, C. Rose, Guidelines and parameter selection for the simulation of progressive delamination, 2008 ABAQUS User's Conference (2008) 1–15.

[33] M. Kenane, M. L. Benzeggagh, Fracture Toughness of Unidirectional Glass / Epoxy Composites Under Fatigue Loading, Composites Science and Technology 3538 (97) (1997) 597–605.